Received: 13 April 2024 | Revised: 29 July 2024 | Accepted: 9 August 2024

https://doi.org/10.1016/j.rpth.2024.102550

ORIGINAL ARTICLE

Antipolyphosphate monoclonal antibodies derived from autoimmune mice

Josepha C. Sedzro[1] | Stephanie A. Smith[1] | Alexander Scott[1] | Yuqi Wang[1] | Richard J. Travers[2] | Rachel Hemp[1] | Chase N. Morse[1] | James H. Morrissey[1]

[1]Department of Biological Chemistry, University of Michigan Medical School, Ann Arbor, Michigan, USA

[2]Department of Biochemistry, University of Illinois at Urbana-Champaign, Urbana, Illinois, USA

Correspondence
James H. Morrissey, Department of Biological Chemistry, University of Michigan Medical School, 4301B MSRB III, 1150 West Medical Center Drive, Ann Arbor, MI 48109-5606, USA.
Email: jhmorris@umich.edu

Present addresses
Alexander Scott, Pfizer, Inc, Chesterfield, Missouri, USA. Yuqi Wang, AbbVie, Worcester, Massachusetts, USA.
Richard J. Travers, Department of Medicine, Division of Hematology Oncology, Tufts Medical Center, Boston, Massachusetts, USA.
Chase N. Morse, Department of Medicinal and Biological Chemistry, The University of Toledo, Toledo, Ohio, USA.

Handling Editor: Dr Carsten Depperman

Abstract

Background: Inorganic polyphosphates (polyPs) are linear chains of phosphates that accelerate blood clotting. Targeting polyP *in vivo* has been shown to reduce thrombosis.

Objectives: To identify and characterize anti-polyP monoclonal antibodies that could be used as analytical tools and as antithrombotic agents.

Methods: Hybridomas were prepared from spleen cells from autoimmune NZBWF1/J female mice and screened for anti-polyP antibodies. Antibodies that bound polyP using enzyme-linked immunosorbent assay and pull-down assays were further characterized with plate binding, surface plasmon resonance, and plasma-based clotting assays. Antithrombotic potential was evaluated in a murine ferric chloride–induced carotid artery thrombosis model.

Results: Of 4 antibodies that bound polyP in our pull-down assay, 2 (PP2069 and PP2099) were available for further characterization. While analyzing these anti-polyP antibodies, we found secretory leukocyte peptidase inhibitor (SLPI) to be a common contaminant of these antibodies and that SLPI binds polyP. We removed SLPI quantitatively from our purified immunoglobulin G. Both PP2069 and PP2099 immunoglobulin G displayed high affinity for polyP but also bound to other polyanions such as DNA, heparin, and certain other glycosaminoglycans, indicating limited specificity. Both antibodies inhibited polyP-initiated plasma clotting *in vitro*. When tested *in vivo* in a mouse thrombosis model, however, neither PP2069 nor PP2099 exhibited a significant antithrombotic effect.

Conclusion: Autoimmune mice spontaneously produce antibodies against polyP. The 2 examples of anti-polyP monoclonal antibodies studied here not only bound to polyP with high affinity but also cross-reacted with DNA and heparin. Neither antibody protected against thrombosis in a mouse model, but they might have some utility for *in vitro* studies of polyP.

KEYWORDS
antibodies, autoantibodies, mice, monoclonal, polyphosphate, thrombosis

Essentials

- Goal was to raise antipolyphosphate antibodies and test their antithrombotic potential.
- Two monoclonal antibodies against polyphosphate were raised using autoimmune mice.
- Both antibodies bound well to polyphosphate and inhibited its clotting activity *in vitro*.
- Neither antibody protected against thrombosis *in vivo* in a mouse model.

1 | INTRODUCTION

Antithrombotic therapy remains a challenge in clinical practice due to the need for effective anticoagulant agents without major bleeding side effects [1]. Polyphosphate (polyP) has emerged as a novel potential target for antithrombotic therapy [2]. PolyP, which consists of linear polymers of inorganic phosphates, is secreted in significant quantities when platelets and mast cells are activated [3,4] and can also be released by infectious microorganisms [5]. Our laboratory and others have shown that polyP is potently procoagulant, activating the contact pathway [6,7], accelerating factor (F)V and FXI activation [8,9], enhancing fibrin clot structure [10,11], and blocking tissue factor inhibitor pathway anticoagulant activity [6,12].

Knocking down polyP expression in platelets protects mice from experimentally induced thrombosis [13], while platelets from humans with Hermansky–Pudlak syndrome (which lack dense granules where polyP is stored) are deficient in supporting blood clotting reactions [6,7]. Consequently, novel polyP inhibitors have been developed and demonstrated to have antithrombotic efficacy in animal models. In 2012, Jain et al. [14] reported that cationic poly(amidoamine) dendrimers (which block polyP procoagulant activity *in vitro*) exhibit antithrombotic activity in mice using a ferric chloride ($FeCl_3$)-induced carotid artery injury model. Also in 2012, our laboratory reported that several polyP inhibitors (including cationic poly(amidoamine) dendrimers) are thromboprotective in mouse models of arterial and venous thrombosis [15]. However, the inhibitors used in those 2012 studies exhibit significant toxicity. In 2014, we reported a novel, cationic dendrimer-like compound with very low toxicity that blocks polyP procoagulant activity *in vitro* and is antithrombotic *in vivo* in mice [16], albeit with some bleeding side effects. More recently, we reported a new generation cationic dendrimer-like compound that protects mice against venous and arterial thrombosis, with essentially no bleeding side effects [17].

Although these dendrimer-like polyP inhibitors are safe and effective in mouse models, they are likely to be relatively short-acting, since other members of this class of compound have circulating half-lives under 40 minutes [18]. We postulated that, if it were possible to generate blocking monoclonal antibodies against polyP, they might be effective polyP inhibitors but with much longer circulating half-lives compared with dendrimer-like polyP inhibitors [19].

In the present study, we sought to identify and characterize anti-polyP monoclonal antibodies as novel agents for blocking polyP procoagulant activity. We now report that, using NZBWF1/J autoimmune mice [20], we were successful in identifying hybridoma lines that secrete anti-polyP antibodies. *In vitro*, 2 of these antibodies (PP2069 and PP2099) bound well to polyP and effectively blocked polyP-induced plasma clotting. Despite these promising *in vitro* results, neither antibody conferred protection against $FeCl_3$-induced thrombosis in a mouse carotid artery injury model. PP2069 and PP2099 may, however, be useful tools for some *in vitro* studies of polyP. Furthermore, the fact that they arose spontaneously in aged NZBWF1/J mice raises the possibility that anti-polyP antibodies may be a feature of some autoimmune disorders, a concept that will require future investigation.

2 | METHODS

2.1 | Materials

Materials were from the following suppliers: Streptavidin-coated 96-well plates, 2-mL Pierce centrifuge columns, Pierce High-Capacity Streptavidin Agarose, horseradish peroxidase (HRP) conjugated to streptavidin (strep-HRP), 1-Step ultra 3,3′,5,5′-tetramethylbenzidine (TMB)–enzyme-linked immunosorbent assay (ELISA) substrate solution, Gibco Hybridoma-SFM, and sterile phosphate-buffered saline (PBS), Thermo Fisher Scientific; high-binding and medium-binding 96-well polystyrene microplates, Corning; streptavidin-conjugated Biacore sensor chips (Sensor Chip SA), Cytiva; HemosIL Recombi-PlasTin 2G, Instrumentation Laboratories; citrated, pooled normal plasma, George King Bio-Medical; control immunoglobulin G (IgG) purified from mouse serum, heparan sulfate sodium salt from bovine kidney, chondroitin sulfate A sodium salt from bovine trachea, chondroitin sulfate B sodium salt from porcine intestinal mucosa, chondroitin sulfate C sodium salt from shark cartilage, microbial hyaluronic acid sodium salt, total yeast RNA (from *Candida utilis*) Sigma; pharmaceutical grade heparin sodium injection solution (10,000 USP units/mL), Mylan Pharmaceuticals; and bovine thrombin, BioPharm Laboratories.

Salmon testis DNA (Sigma) was sheared by dissolving in water at 20 mg/mL and passing 10 to 20 times through a 25-gauge needle, followed by 3 rounds of 1-minute sonication at 50% amplitude

(QSonica model Q125 sonicator). Phospholipid vesicles (80% 1-palmitoyl-2-oleoyl-*sn*-glycero-3-phosphocholine/20% 1-palmitoyl-2-oleoyl-*sn*-glycero-3-L-serine) were prepared by sonication [21], using phospholipids from Avanti Polar Lipids. The recombinant polyP-binding domain of *Escherichia coli* exopolyphosphatase (PPXbd) was produced as described [8], for use as a positive control for blocking polyP clotting activity [15].

polyP$_{long}$, a heterogeneous preparation of long-chain polyP with a modal polymer length of 1090 phosphates and a range of 200 to 1300 phosphates, was prepared as described [22]. Biotin-polyP$_{long}$ was prepared via covalently end-labeling polyP$_{long}$ with amine-diethylene glycol-biotin [22]. Biotin-polyP$_{1075}$, a narrowly size-fractionated, biotinylated polyP preparation was isolated from biotin-polyP$_{long}$ by preparative polyacrylamide gel electrophoresis (PAGE) as previously described [12], but using a Bio-Rad model 491 Prep Cell with continuous fraction elution. Biotin-polyP$_{1075}$ had a modal length of 1075 phosphates and a range of 1020 to 1145 phosphates. PolyP lengths were estimated as described [23]. Molar polyP concentrations are reported as the concentration of phosphate monomers.

2.2 | Initial production and purification of anti-polyP monoclonal antibodies

Generation of mouse hybridoma lines secreting putative anti-polyP antibodies, and initial production and purification of IgG, were carried out in the laboratory of Charles and Naomi Esmon at the Oklahoma Medical Research Foundation as follows (using procedures approved by the Institutional Animal Care and Use Committee). Spleen cells from unimmunized, 6-month-old female NZBWF1/J mice were fused with P3X63AG8-653 cells to create hybridomas [24]. Hybridoma supernatants were screened for polyP-binding antibodies using an ELISA in which biotin-polyP$_{long}$ was immobilized on streptavidin-coated microwell plates, after which wells were incubated with diluted hybridoma culture supernatants, washed, incubated with HRP-conjugated goat anti-mouse IgG, then washed again and incubated with TMB-ELISA substrate. Nearly 40 hybridomas were putatively identified as polyP-binding using this ELISA assay and were subcloned in the Esmon laboratory. The Esmon laboratory produced milligram quantities of IgG from these hybridomas using large-scale cell culture in serum-free media (Gibco Hybridoma-SFM), supplemented with 0.25 ng/mL human interleukin-6 (IL-6) (Miltenyi Biotec) to increase IgG production [25]. IgG was initially isolated in the Esmon laboratory from spent culture supernatants using chromatography on mercaptoethylpyridine (MEP) HyperCel resin (Pall Corporation). Briefly, the starting material was pumped over an MEP HyperCel column equilibrated with tris-buffered saline (TBS) (100 mM NaCl, 50 mM Tris-HCl buffer, pH 7.5). Columns were then washed with 4-column volumes of TBS, after which the IgG was eluted with 50 mM sodium acetate buffer, pH 4.0. When the Esmons closed their laboratory upon their retirement, the hybridoma lines and IgG preparations were transferred to us. Subsequent analyses reported in this paper were carried out in our laboratory.

2.3 | Characterization of IgG subclass and IgG purity

PP2069 and PP2099 were identified as IgG2a, kappa antibodies using the Pierce Rapid Isotyping Kit-Mouse (Thermo Fisher Scientific). IgG concentrations in milligrams per milliliter were quantified by A_{280} (extinction coefficient, 1.37). IgG purity was assessed by sodium dodecyl sulfate (SDS)–PAGE using 4% to 20% Mini-PROTEAN TGX Precast Gels (Bio-Rad), stained with Coomassie G-250 (GelCode Blue; Thermo Fisher Scientific).

2.4 | Additional IgG purification and production

Selected IgG preparations from the Esmon laboratory were further purified on an ÄKTA Start using protein A affinity chromatography (HiTrap Protein A HP; Cytiva), according to the manufacturer's instructions. After the protein A chromatography step, any remaining low-molecular weight (MW) contaminants were removed by repeated centrifugal ultrafiltration using Amicon Ultra-4 spin columns (50 kDa MW-cutoff; Sigma Aldrich) as follows. IgG preparations PP2069, PP2099, and PP2070 (pooled eluted fractions) were concentrated by centrifugal ultrafiltration (4500 × *g* for 5 minutes), then diluted 3-fold with high-salt HBS (HEPES-buffered saline) (1 M NaCl, 30 mM 4-[2-hydroxyethyl]-1-piperazineethanesulfonic acid [HEPES] pH 7.4, 0.1% NaN_3) and centrifuged in the same column again. After 3 rounds of such centrifugal concentration using high-salt HBS, the samples were subjected to 3 rounds of centrifugal concentration using low-salt HBS (50 mM NaCl, 30 mM HEPES pH 7.4, 0.1% NaN_3).

Some additional quantities of PP2069 IgG were produced in mice (as ascites) at the University of Michigan Hybridoma core. IgG was precipitated from ascites fluid with 50% saturated ammonium sulfate, redissolved and dialyzed, then further purified on an ÄKTA Start using Pierce Protein G Chromatography Cartridges (Thermo Fisher Scientific) according to the manufacturer's instructions.

2.5 | polyP pull-down assays

polyP beads were prepared by mixing 1 mL of 200 mM biotin-polyP$_{1075}$ in TBS plus 1 mM EDTA (TBSE) with 1-mL damp streptavidin-agarose beads in a 2-mL spin column and rotating at ambient temperature for 10 minutes. Beads were collected by centrifugation (1000 × *g* for 30 seconds), then washed sequentially by centrifugation with TBSE, 0.5 M NaCl, and then TBSE again, in which the beads were stored. For pull-down procedures, 50 µL of 100 µg/mL IgG in TBSE was mixed with 150-µL damp polyP beads in 2-mL spin columns and rotated at ambient temperature for 30 minutes, after which the flow-through was collected by centrifugation. Beads were washed 3 times with 500 µL TBSE, then suspended in 50 µL of 0.5 M NaCl and rotated for 5 minutes. Eluates were collected by centrifugation. PP2070 came from the same hybridoma fusion as the other monoclonal antibodies in this study, but as it did not bind to polyP in our pull-down assays, it was used as a negative control in some assays.

2.6 | Plasma clotting assays

Ability of IgGs to inhibit polyP-initiated clotting was assessed using a microplate-based, modified activated partial thromboplastin time clotting assay as described [21], except that immediately prior to initiating the assays, 3-μM $polyP_{long}$ was preincubated for 15 minutes at ambient temperature with varying concentrations of IgG or PPXbd in a solution containing 0.1% bovine serum albumin (BSA), 30-μM phospholipid vesicles, and 20 mM HEPES pH 7.4. Clotting assays were then carried out using 50 μL of this preincubated solution as described [21]. The final polyP concentration was 1 μM.

A modified prothrombin time clotting assay was carried out using a thromboplastin reagent (HemosIL RecombiPlasTin 2G) diluted 1/1000-fold in a solution containing 30-μM phospholipid vesicles, 100 mM NaCl, 20 mM HEPES pH 7.4, 0.1% BSA and 0.02% NaN_3. To this solution, an equal volume of 12 μM IgG diluted in the same buffer was added and incubated 15 minutes at ambient temperature, after which 50 μL of this preincubated solution was mixed with 50 μL pooled normal plasma in the wells of a medium-binding microplate and incubated for 3 minutes at 37 °C. Clotting was initiated by adding 50 μL prewarmed 25 mM $CaCl_2$ and time to initial polymerization was determined by monitoring A_{405} on a SpectraMax microplate reader (Molecular Devices) as described [26]. The final IgG concentration was 2 μM and final RecombiPlasTin dilution was 1/6000.

2.7 | Plate binding assays

Wells of high-binding microplates were coated overnight with 4 μg/mL PP2069 IgG or 8 μg/mL PP2099 IgG in TBS, then washed 3 times with HNKE buffer (20 mM HEPES pH 7.4, 140 mM NaCl, 5 mM KCl, 5 mM EDTA) plus 0.1% Tween-20 (HNKE-Tween), blocked 2 hours with 5% BSA in HNKE, washed 3 times with HNKE-Tween, and then incubated for 2 hours at ambient temperature with various biotin-$polyP_{long}$ concentrations in HNKE-Tween plus 2% BSA. After washing with HNKE-Tween, wells were incubated 2 hours with 1 μg/mL of strep-HRP in HNKE-Tween plus 2% BSA and then washed 3 times with HNKE-Tween, after which 60 μL TMB-ELISA substrate was added and incubated for 5 minutes. Wells then received 60 μL of 1N sulfuric acid and A_{450} was measured.

To evaluate binding competition, the polyP incubation step of this assay employed a fixed polyP concentration (250 nM biotin-$polyP_{long}$ for PP2069 or 400 nM biotin-$polyP_{long}$ for PP2099) plus varying concentrations of glycosaminoglycans (GAGs), DNA, or RNA. International Units of heparin were converted into mass concentrations assuming a specific activity of 200 IU/mg [27].

2.8 | $FeCl_3$-induced thrombosis in mouse carotid arteries

Antithrombotic activity of PP2069 and PP2099 IgGs was evaluated in approximately 10-week-old male and female C57BL/6J mice using $FeCl_3$-induced injury to carotid arteries [16]. Procedures were approved by the University of Michigan Institutional Animal Care and Use Committee.

2.9 | Surface plasmon resonance

Surface plasmon resonance (Biacore T200 instrument; Cytiva) was used to quantify IgG binding to biotin-$polyP_{1075}$ immobilized on streptavidin sensor chips as described [17], except that the running buffer was HNKE plus 0.005% P20 surfactant. Dissociation constant (K_d) values were derived by plotting the maximal (steady-state) response units versus IgG concentration, to which the single-site ligand binding equation was fitted using nonlinear regression.

2.10 | Statistical analysis

Statistical analyses were performed with Prism version 10.0 (GraphPad Software). In general, 1-way analysis of variance was used as a statistical test of variance with Tukey's multiple comparison. For the Kaplan–Meier curves, log-rank (Mantel-Cox) and Gehan–Breslow–Wilcoxon's tests were used as statistical test of variance.

3 | RESULTS

3.1 | Identification of anti-polyP IgGs

NZBWF1/J mice spontaneously develop an autoimmune disease that resembles human systemic lupus erythematosus (SLE), including high levels of antinuclear antibodies [20]. We therefore hypothesized that these mice might develop self-reactive antibodies toward polyP. As described in Methods, hybridoma lines were prepared from spleen cells of aged, unimmunized NZBWF1/J female mice. Culture supernatants from these hybridomas were then screened using an ELISA in which long-chain polyP was immobilized on wells to capture anti-polyP antibodies from the culture supernatants. This initial screening ELISA identified 38 hybridoma lines that appeared to secrete polyP-binding antibodies. These hybridomas were grown in large-scale cultures, from which initial IgG preparations were isolated using a rapid, relatively inexpensive chromatography method (MEP HyperCel). When resolved by SDS-PAGE, most of the antibody preparations had lower-MW contaminants, indicating they were only partially pure at this stage (Supplementary Figure S1).

Surprisingly, some preparations of these putative anti-polyP antibodies (eg, PP2071) gave positive signals in the polyP screening ELISA yet exhibited little or no visible IgG band on SDS-PAGE (Supplementary Figure S1). Accordingly, we employed a pull-down assay using polyP-coated beads to reveal which protein(s) in the various antibody preparations actually bound to polyP. When the high-salt-eluted proteins were resolved by SDS-PAGE (Figure 1), a band with the correct MW for IgG was obtained from 4 of the

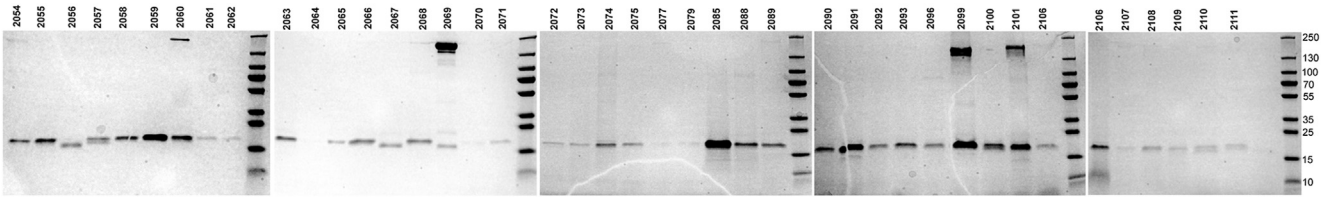

FIGURE 1 Polyphosphates (polyPs) pull-downs reveal which proteins in the immunoglobulin G (IgG) preparations bind to polyP. A single batch of each IgG preparation was randomly selected for polyP pull-down assay. After incubation with antibody solution, the polyP beads were subsequently washed and then treated with 0.5 M NaCl to release any specifically bound proteins. One-fourth of each eluted sample was resolved by sodium dodecyl sulfate–polyacrylamide gel electrophoresis (4%-20% gradient gels) under nonreducing conditions and then stained with Coomassie. (Some gels tore during processing and were reassembled.) Molecular weight (MW) standards in kDa are indicated on the right. As can be seen from the staining patterns, a prominent protein migrating with an apparent MW of approximately 17 KDa was pulled down by polyP beads and eluted by 0.5 M NaCl from almost all the preparations. In contrast, a protein band of the correct size for IgG (150 kDa) was pulled down and eluted from only 4 of the antibody preparations: PP2060, PP2069, PP2099, and PP2101.

antibody preparations (PP2060, PP2069, PP2099, and PP2101), demonstrating that only these 4 IgGs were polyP-binding. Notably, almost all the lanes also showed a prominent approximately 17-kDa protein band, indicating the presence of a common polyP-binding contaminant in most of the preparations.

3.2 | Identification of the common polyP-binding contaminant as secretory leukocyte peptidase inhibitor

A preparation of PP2059 IgG similar to that shown in Supplementary Figure S1 was subjected to polyP pull-down, and the 0.5 M NaCl eluate was resolved on nonreduced SDS-PAGE. The single band migrating with an apparent MW of approximately 17 kDa was cut from the gel and submitted to the University of Michigan Proteomics and Peptide Synthesis Core for identification. As shown in Supplementary Figure S2, the predominant protein in the sample was identified as mouse secretory leukocyte peptidase inhibitor (SLPI) (UniProt ID: P97430). SLPI (also known as antileukoproteinase) is a small (11.7 kDa), basic (isoelectric point (pI), 8.7), highly disulfide-bonded protein that migrates somewhat anomalously on non-reduced SDS-PAGE [28]. Since SLPI binds heparin with high affinity [29–31], it is perhaps not surprising that SLPI is also a polyP-binding protein. SLPI has previously been reported as a prominent contaminant of a murine monoclonal antibody produced in serum-free culture [32].

3.3 | Further purification of anti-polyP IgGs

Given that SLPI binds to polyP, its presence in our IgG preparations would confound assessments of polyP-IgG interactions. This is especially true given SLPI's much smaller size than IgG, meaning that even low mass concentrations of SLPI could still be significant on a molar basis. We therefore sought to fully purify the 4 polyP-binding antibodies. Unfortunately, we were unable to recover viable frozen hybridoma cells for PP2060 or PP2101, so we focused our remaining attention on antibodies PP2069 and PP2099. Of these 2, we found that the PP2099 hybridoma cells had microbial contamination that, to date, we have been unable to remove, so at present we are only able to grow the PP2069 hybridoma line. Accordingly, we produced and purified additional quantities of PP2069 IgG as described in Methods, and we also focused on removing contaminating proteins from our existing stocks of both PP2069 and PP2099 IgG. As shown in Supplementary Figure S3, the contaminating lower-MW bands were successfully removed from existing IgG preparations using protein A affinity chromatography followed by repeated centrifugal ultrafiltration.

We confirmed the ability of purified PP2069 and PP2099 IgG to interact with polyP in pull-down assays using biotinylated long-chain polyP immobilized on streptavidin beads. As can be seen in Figure 2A, little of the PP2069 and PP2099 IgGs were found in the flow-through, with most of the IgG signal appearing in the 0.5 M NaCl eluate. IgG from PP2070, another hybridoma line from the same fusion, was an example of an antibody that did not bind to polyP, as it was seen only in the flow-through and not the 0.5 M NaCl eluate in pull-downs (Figure 2B). A commercial preparation of whole IgG from mouse serum showed the same negative response in the polyP pull-down assay (Figure 2B), confirming the specificity of the pull-down assay for polyP binding. This experiment also documents the purity of the preparations of PP2069, PP2099, and PP2070 IgGs used in the remainder of our studies.

3.4 | Affinity and specificity of antibodies PP2069 and PP2099 for binding to polyP

We used a microplate-based binding assay to measure the affinity of antibodies PP2069 and PP2099 for polyP (Figure 3A, B), yielding K_d values for polyP binding to PP2069 and PP2099 IgG of 928 ± 164 nM and 850 ± 146, respectively. These K_d values are expressed in terms of the phosphate monomer concentration of polyP.

To further explore the interaction between antibody PP2069 and polyP, we performed surface plasmon resonance analysis in which varying PP2069 IgG concentrations were flowed over immobilized,

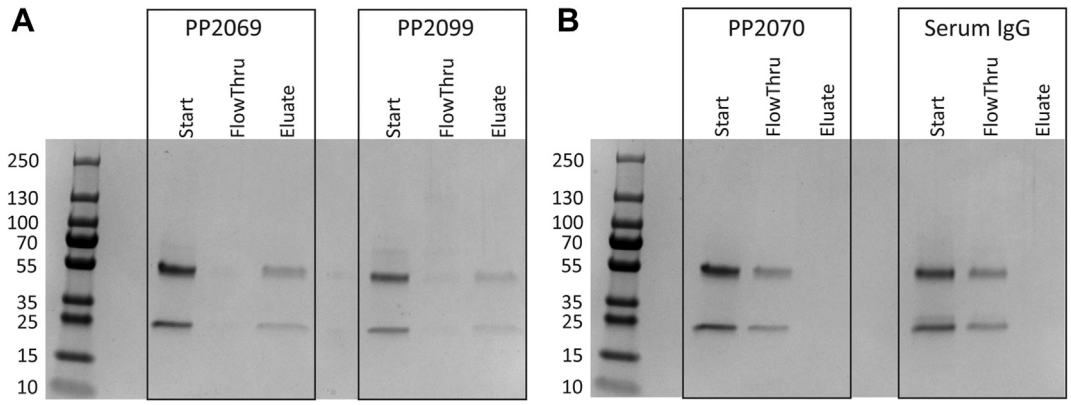

FIGURE 2 Pull-down assay for binding of purified immunoglobulin G (IgG) to polyphosphate (polyP). Polyphosphate beads were incubated with 100 μg/mL of the indicated purified IgG preparations, after which the flow-through and 0.5 M NaCl eluates were collected using spin columns. Reduced samples were resolved on sodium dodecyl sulfate–polyacrylamide gel electrophoresis and stained with Coomassie. Representative pull-downs are shown for (A) PP2069 and PP2099 and (B) PP2070 and whole IgG from mouse serum. Note the expected IgG bands at approximately 50 and 25 kDa, and the absence of other contaminating bands.

biotin-polyP$_{1075}$, and the maximal (steady-state) response unit values were plotted versus IgG concentration (Figure 3C, D). Fitting the single-site ligand binding equation to the binding isotherm yielded a K_d value of 927 ± 17 nM (in this case, expressed in terms of IgG concentration).

Since polyP is highly anionic and has a simple, repeating structure, it seems likely that binding of anti-polyP antibodies to polyP will be dominated by electrostatic interactions. This raises the question of binding specificity, so we assessed the ability of other anionic, biological polymers to compete with polyP for binding to PP2069 or PP2099 using

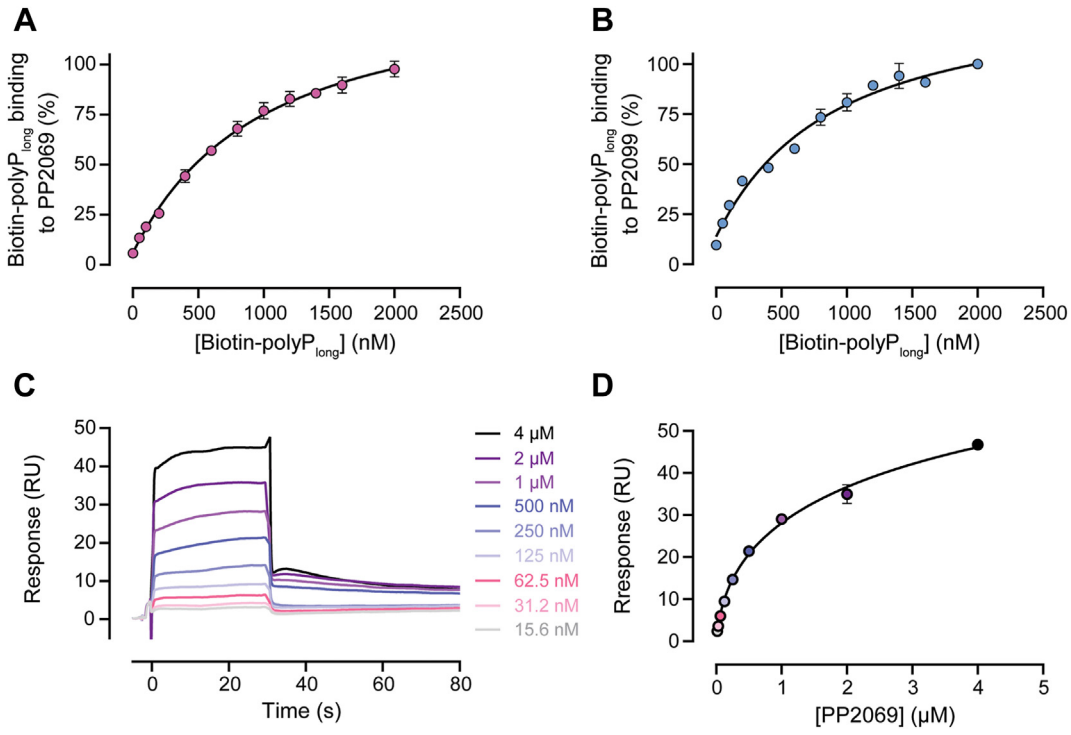

FIGURE 3 Affinity of antibodies PP2069 and PP2099 for polyphosphate (polyP). (A, B) polyP binding to immobilized immunoglobulin G (IgG). Wells were coated with (A) PP2069 or (B) PP2099 IgG, then incubated with varying concentrations of biotin-polyP$_{long}$, after which bound biotin-polyP$_{long}$ was detected using horseradish peroxidase–conjugated streptavidin. Signals were normalized to the amount of binding observed with the highest biotin-polyP concentration and plotted versus polyP concentration. Dissociation constant values were obtained by fitting the single-site ligand binding equation. (C, D) Surface plasmon resonance analysis of PP2069 IgG binding to polyP. (C) Representative surface plasmon resonance sensorgrams in which varying concentrations of PP2069 IgG were flowed over immobilized biotin-polyP$_{1075}$. (D) Binding isotherm for PP2069 IgG, in which the mean maximal steady-state response unit (RU) values are plotted versus PP2069 IgG concentration, fitted with the single-site ligand binding equation. Dissociation constant was 927 ± 17 nM. Data points in panel A, B, and D are mean ± SE of the mean (n = 4). Panel C shows a representative sensorgram. PolyP$_{long}$, long-chain polyphosphate.

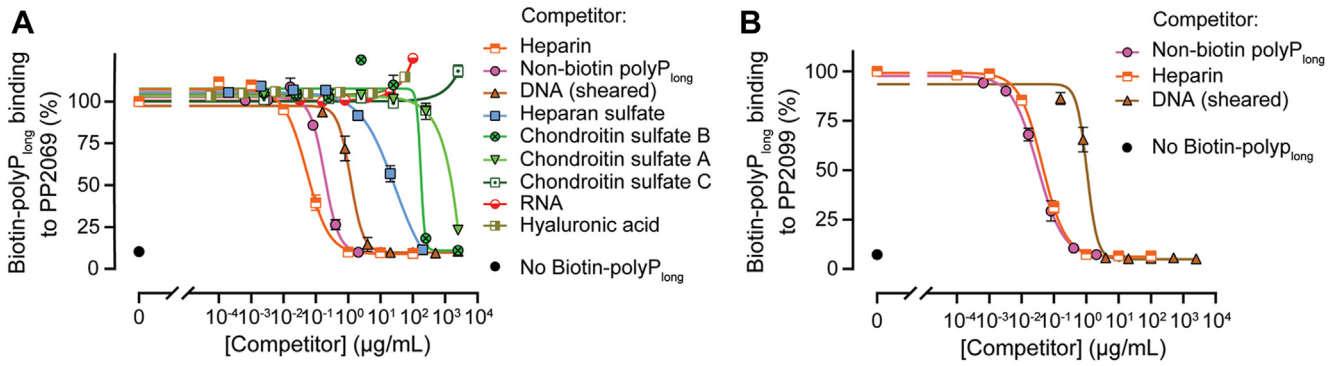

FIGURE 4 Ability of glycosaminoglycans, DNA or RNA to compete with polyP for antibody binding. Wells were coated with (A) PP2069 or (B) PP2099 immunoglobulin G, then incubated with a fixed concentration of biotin-polyP$_{long}$ plus varying concentrations of the indicated glycosaminoglycans, sheared salmon testis DNA or yeast RNA, after which bound biotin-polyP$_{long}$ was detected using horseradish peroxidase–conjugated streptavidin. Signals were normalized to the amount of binding observed with no competitor (set to 100%) and plotted versus competitor concentration. IC_{50} values (summarized in the Table) were obtained by fitting a sigmoidal, 4-parameter logistic equation. In all panels, data are mean ± SE of the mean (n ≥3). PolyP$_{long}$, long-chain polyphosphate.

our plate-based binding assay in which IgGs were immobilized on microwell plates (Figure 4, with half-maximal inhibitory contration [IC_{50}] values in the Table). We evaluated the whole panel of competitors for binding to PP2069, but as we had only limited amounts of purified PP2099 IgG available, we performed selective evaluation of the competitors with that antibody.

As a positive control, we examined competition between non-biotinylated polyP$_{long}$ and biotin-polyP$_{long}$ for antibody binding, observing IC_{50} values for unlabeled polyP of 0.20 ± 0.03 μg/mL for PP2069 and 0.032 ± 0.005 μg/mL for PP2099. In comparison, the highly anionic GAG, heparin, competed with biotin-polyP$_{long}$ for binding to these antibodies with IC_{50} values of 0.054 ± 0.007 μg/mL for PP2069 and 0.043 ± 0.002 μg/mL for PP2099. Thus, heparin was an approximately 3.7-fold better competitor than polyP for binding to PP2069 but competed about equally for binding to PP2099. Heparan sulfate, which is less intensely anionic than heparin, competed with polyP for binding to PP2069 with an IC_{50} value that was more than 600-fold higher than that of heparin (and 175-fold higher than that of free polyP), consistent with the notion that electrostatic interactions are highly important in binding polyP to PP2069.

TABLE IC_{50} values of various competitors for binding of biotin-polyP$_{long}$ to immobilized IgG in a microplate-based binding assay.

Competitor	PP2069 IgG IC_{50}, μg/mL[a]	PP2099 IgG IC_{50}, μg/mL[a]
Nonbiotinylated polyP$_{long}$	0.20 ± 0.03	0.032 ± 0.005
Heparin	0.054 ± 0.007	0.043 ± 0.002
Heparan sulfate	35 ± 14	Not tested
Chondroitin sulfate A	4390 ± 2860[b]	Not tested
Chondroitin sulfate B	117 ± 26	Not tested
Chondroitin sulfate C	N.D.C.	Not tested
Hyaluronic acid	N.D.C.	Not tested
DNA	4.8 ± 3.6	0.98 ± 0.09
RNA	N.D.C.	Not tested

IgG, immunoglobulin G; N.D.C., no detectable competition; polyP$_{long}$, long-chain polyphosphate.

[a]IC_{50} values (half-maximal inhibitory concentrations) are mean ± SE of the mean ($n \geq 3$).

[b]The weak competition exhibited by chondroitin sulfate A resulted in considerable variation from assay to assay, hence the high SE.

We tested other anionic GAGs (chondroitin sulfate A, B, and C, and hyaluronic acid) for competition with polyP for binding to PP2069, but of these only chondroitin sulfate A and B exhibited measurable competition over the concentration range we could test. For chondroitin sulfate B, the IC_{50} value was some 2000-fold higher than that of heparin, and about 585-fold higher than that of free polyP. The IC_{50} for chondroitin sulfate A was 80,000-fold higher than that of heparin, and 22,000-fold higher than that of free polyP.

Using sheared salmon testis DNA as a competitor for both antibodies, we found that DNA had an IC_{50} value of 4.8 ± 3.6 μg/mL toward PP2069 and 0.98 ± 0.09 μg/mL toward PP2099. Thus, for PP2069, the IC_{50} value for DNA is about 90-fold higher than that of heparin, and about 24-fold higher than that of free polyP, while for PP2099, the IC_{50} value for DNA is approximately 23-fold higher than that of heparin and about 30-fold higher than that of free polyP. This demonstrates that both PP2069 and PP2099 bind to DNA, albeit with lower affinity than their binding to polyP. On the other hand, we observed no detectable competition between yeast RNA and polyP for binding to PP2069.

Altogether, our results showed that heparin potently competes with polyP for binding to PP2069 and PP2099, and that DNA also competes significantly with polyP for binding to these antibodies, albeit with reduced potency. This is consistent with the idea that the interaction of these IgGs with polyP is dominated by electrostatic interactions and that they are not highly specific for polyP. In fact, both antibodies bound at least as well to heparin as they did to free, long-chain polyP.

3.5 | PP2069 and PP2099 inhibit polyP procoagulant activity

We assessed the ability of PP2069 and PP2099 to block the procoagulant activity of long-chain polyP in a modified activated partial thromboplastin time clotting assay (Figure 5A). When clotting was triggered by 1 μM $polyP_{long}$, PP2069 and PP2099 IgGs dose-dependently prolonged the clot times, reaching 447 ± 25 seconds and 440 ± 20 seconds with 2 μM PP2069 or PP2099 IgG, respectively (Figure 5B). Thus, 2 μM PP2069 or PP2099 IgG fully inhibited the procoagulant activity of long-chain polyP. The polyP-binding protein, PPXbd, also completely blocked polyP clotting activity at 2 μM, while the non–polyP-binding antibody, PP2070, had little to no effect on polyP-initiated clotting (Figure 5B).

To test whether PP2069 or PP2099 IgG nonspecifically inhibit plasma clotting (eg, by binding to anionic phospholipids), we also tested their effect in a modified prothrombin time assay in which the thromboplastin reagent was diluted to yield a 30 to 40 second time (Figure 5C). When tested at 2 μM IgG, neither PP2070, PP2069, nor PP2099 prolonged the clotting time in this assay (Figure 5D). This confirms that PP2069 and PP2099 IgG specifically abrogate polyP-triggered clotting and do not have a general anticoagulant effect.

3.6 | Neither PP2069 nor PP2099 IgG protect mice against thrombosis

Given that PP2069 and PP2099 block polyP procoagulant activity *in vitro*, and given previous demonstrations that blocking polyP *in vivo* can protect against experimentally induced thrombosis [15–17,33], we assessed the antithrombotic activity of PP2069 and PP2099 IgG *in vivo* using a mouse model of $FeCl_3$-induced injury to the carotid artery. We administered bolus doses of PP2069 IgG at 10 mg/kg or 40 mg/kg body weight, or of PP2099 IgG at 10 mg/kg body weight, followed by induction of thrombosis. Blood flow ceased in carotid arteries of control mice (PBS carrier) within 400 seconds after removal of the $FeCl_3$-saturated filter papers (Figure 6). Administration of neither PP2069 IgG (Figure 6A, C) nor PP2099 IgG (Figure 6B, C) significantly prolonged the time to occlusion compared with mice injected with PBS alone or with whole mouse serum-derived IgG.

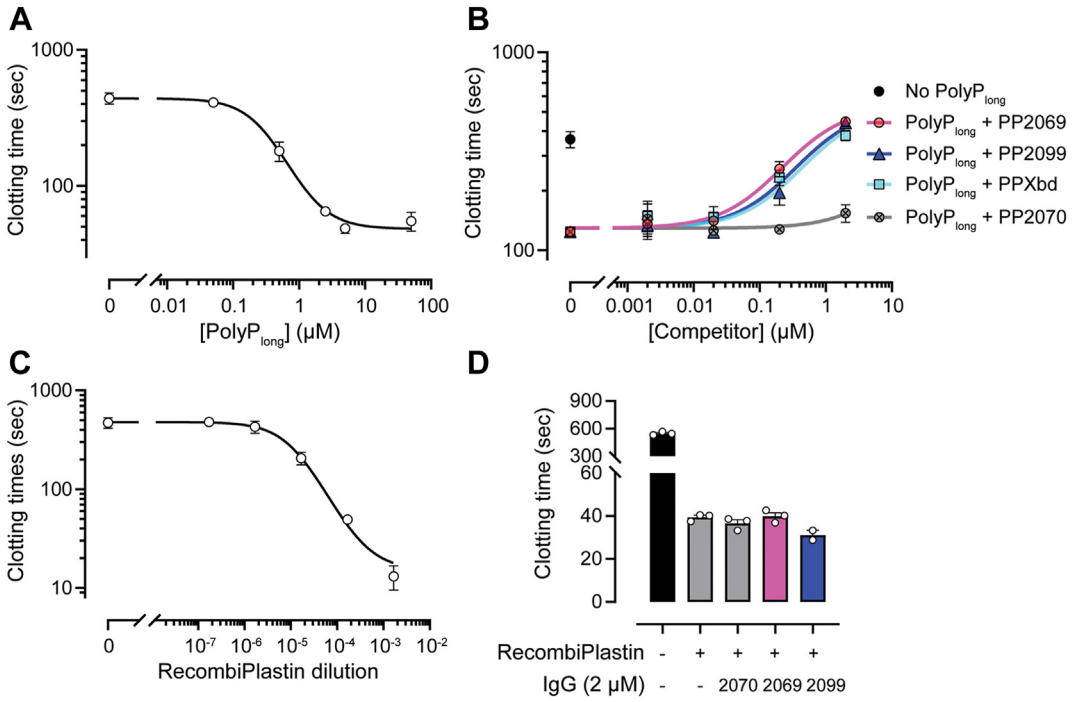

FIGURE 5 Antipolyphosphate immunoglobulin G (IgG) inhibits polyphosphate (polyP) clotting activity. (A, B) Modified activated partial thromboplastin time clotting assay in which plasma clotting was triggered by $polyP_{long}$. (A) Dependence of plasma clotting time on $polyP_{long}$ concentration. Clotting time was 124 ± 7 seconds with 1 μM $polyP_{long}$, and 364 ± 34 seconds without polyP. (B) Ability of PP2069 IgG, PP2099 IgG, or PPXbd to prolong clotting of plasma triggered by 1 μM $polyP_{long}$ (with PP2070 IgG included as a negative control). (C, D) Lack of effect of PP2069 or PP2099 IgG on tissue factor-initiated clotting of plasma (modified prothrombin time [PT] assay). (C) Dependence of plasma clotting time on dilution of the clotting initiator, RecombiPlasTin. For subsequent tests, we chose a 6000-fold dilution of RecombiPlasTin, yielding a mean clotting time of 39 ± 1.7 seconds. The clotting time without RecombiPlasTin was 548 ± 19 seconds. (D) Lack of influence of PP2070, PP2069, or PP2099 IgG on tissue factor-initiated clotting. When included in these clotting tests at 2 μM IgG, none of the antibodies prolonged the clotting time. Data in all panels are mean ± SE of the mean (n = 3 except for the experiments in panel D with PP2099, which were repeated twice). $PolyP_{long}$, long-chain polyphosphate.

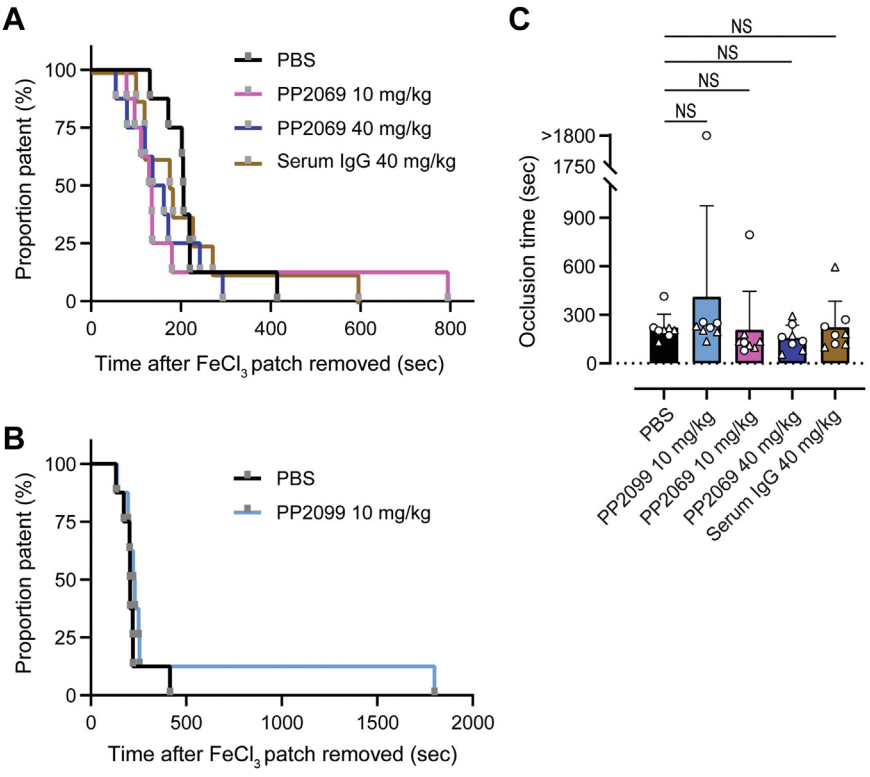

FIGURE 6 Neither PP2069 nor PP2099 immunoglobulin G (IgG) protected mice against experimentally induced thrombosis. (A, B) Mice were injected retro-orbitally with IgG in sterile phosphate-buffered saline (PBS) at the indicated doses (10 or 40 mg/kg body weight), after which thrombosis was triggered in the exposed carotid artery by application of ferric chloride ($FeCl_3$)-soaked filter papers. Blood flow was monitored with a Doppler flow probe. Antibodies were PP2069 or PP2099 IgG, or whole IgG from mouse serum, while the indicated control mice received just sterile PBS. Shown here are Kaplan–Meier curves for administering: (A) PP2069 or serum IgG, or (B) PP2099. (Note that data from the same PBS control animals are plotted in both panels.) (C) Bar graph of occlusion times. Administration of PP2069 IgG at neither 10 nor 40 mg/kg body weight significantly changed the proportion of patent arteries relative to either of the groups of control mice (PBS or serum IgG), nor did administration of PP2099 IgG at 10 mg/kg. For each group, 8 mice were analyzed; open circles represent female mice and open triangles represent males. Data are mean ± SD. NS, not statistically significant.

Thus, while PP2069 and PP2099 IgG blocked polyP clotting activity *in vitro*, they did not confer detectable protection against thrombosis in this model *in vivo*.

4 | DISCUSSION

In this study, we sought to identify antibodies that could specifically target polyP for use *in vitro* and *in vivo*. We and others have previously identified a variety of proteins and other reagents that can be used to detect, label, or inhibit polyP [2,34–36]. Nevertheless, it would be highly desirable to generate specific anti-polyP antibodies, given the many technical advantages that antibodies possess as research tools and therapeutics. The ubiquitous nature and simple structure of polyP suggested that raising antibodies in normal animals might be difficult, so instead we screened for anti-polyP antibodies arising spontaneously in NZBWF1/J autoimmune mice since these animals are known to produce antibodies against other common self-antigens such as nucleic acids. We now report the identification of 4 monoclonal antibodies derived from spleen cells of unimmunized NZBWF1/J mice that recognize polyP. We purified and characterized 2 of these antibodies (PP2069 and PP2099) and documented that they bind to polyP with high affinity. Furthermore, both antibodies effectively blocked the plasma clotting activity of long-chain polyP in a manner very similar to that of PPXbd, a well-known polyP-blocking protein.

Although PP2069 and PP2099 bound with high affinity to polyP and blocked its clotting activity, neither antibody was specific for polyP as both bound to other anionic biological polymers. Competition experiments indicated that PP2069 and PP2099 bound to heparin and, in fact, PP2069 bound almost 4-fold better to heparin than to polyP, while PP2099 bound about equally well to heparin and polyP. These anti-polyP antibodies also interacted with other GAGs such as heparan sulfate, and they bound to DNA, underscoring their lack of specificity toward polyP.

We were disappointed that neither PP2069 nor PP2099 IgG was antithrombotic in a mouse arterial thrombosis model (induced by $FeCl_3$) in spite of blocking polyP clotting activity *in vitro*. In contrast, we and others have shown that PPXbd and several other polyP inhibitors are thromboprotective in this and other animal models of thrombosis [15–17,35]. We do not know why these 2 anti-polyP antibodies failed to be thromboprotective in this model, although one possibility is that binding to heparan sulfate proteoglycans on endothelial cells, and perhaps other anionic biomolecules, may lead to off-target effects and/or sequestration of the antibodies away from polyP. It is possible that these antibodies might protect against thrombosis in other models (ie, triggered by insults other than $FeCl_3$), but this would have to be investigated in further studies.

It is interesting that PP2069 and PP2099 bound to DNA with appreciable affinity. Antibodies against double-stranded DNA are prominent hallmarks of SLE, and indeed testing for anti-DNA antibodies plays an important role in diagnosing, classifying, and

monitoring SLE [37]. We originally chose NZBWF1/J mice because they are a model for SLE and are known to develop anti-DNA antibodies [20]. It is tempting to speculate that anti-polyP antibodies may occur in human SLE (and other human autoimmune conditions), and also to speculate that some of the known anti-DNA antibodies in SLE might cross-react with polyP. It will be interesting to explore these ideas in future studies.

Since these antibodies bound effectively to DNA as well as heparin, they might have utility in studying the function of those polymers. This could be evaluated in future studies, eg, by testing their ability to block heparin's anticoagulant activity or to protect DNA from DNase degradation.

An unexpected technical challenge was the ubiquitous presence of SLPI as a strongly polyP-binding protein that contaminated most of the initial IgG preparations. SLPI has previously been reported to contaminate murine monoclonal antibodies produced in serum-free cell culture [32], and in fact, SLPI expression by mouse myeloma lines was strongly correlated with IgG expression [38]. The hybridoma lines employed in this study were initially cultured in the presence of IL-6 to boost IgG production [25]. IL-6 increases SLPI production by macrophages [39], so it seems possible that including IL-6 in the hybridoma medium also promoted SLPI overaccumulation. And finally, the IgG isolation method for the initial panel of 38 antibodies was MEP HyperCel chromatography, which can be used to purify IgG under appropriate conditions [40]. It would appear that co-purification of SLPI with IgG is a potential caveat to using this method, at least under the chromatography conditions employed.

SLPI is a protease inhibitor that also exhibits potent immunomodulatory and anti-inflammatory activities [28]. SLPI binds heparin with high affinity, and heparin modulates some of SLPI's biological activities [29–31]. We now report that SLPI binds polyP. It is tempting to speculate that polyP may modulate some of SLPI's activities, which we will examine in future studies. We presume that the presence of SLPI gave false-positive signals in the original screening polyP-ELISA, although we have not tested this idea explicitly. Given that SLPI can contaminate murine monoclonal antibodies, and also given its small size (making it easy to overlook by SDS-PAGE unless gradient gels are used), our experience with SLPI is a cautionary tale for anyone using monoclonal antibodies with polyP.

PP2055 is one of the antibodies that gave a positive polyP binding signal in the initial screening ELISA (Supplementary Figure S1), but it failed to bind to polyP in our pull-down assay (Figure 1) and is therefore not an anti-polyP antibody. We note that a 2017 study reported using the PP2055 antibody as a polyP-binding reagent [41], although those authors subsequently published an erratum stating that the results they obtained with it "cannot be confidently interpreted, because they may be confounded by a lack of purity and/or specificity" [41].

In conclusion, our study describes the spontaneous development of polyP-binding antibodies in autoimmune mice that are known to develop an SLE-like condition. We studied 2 of these anti-polyP antibodies in greater detail. Both blocked polyP clotting activity *in vitro*, but this did not translate to antithrombotic efficacy *in vivo*, at least when tested in a $FeCl_3$-induced, arterial thrombosis model. Lack of specificity for polyP has long been a challenge in development of agents to target this highly charged polymer, and indeed neither of these 2 antibodies showed high specificity for polyP. Our study does, however, demonstrate that anti-polyP antibodies can arise spontaneously in autoimmune conditions.

ACKNOWLEDGMENTS

The hybridoma fusions, initial screening for anti-polyP antibodies, and initial antibody production and purification were carried out in the laboratory of Charles and Naomi Esmon at the Oklahoma Medical Research Foundation in Oklahoma City. After the Esmons retired and closed their laboratory, they kindly shipped the existing hybridoma lines and antibody preparations to our laboratory for further analyses. We gratefully acknowledge their contribution to this project.

FUNDING

This study was supported by grants R35 HL135823, R35 HL171334, and UM1 HL120877 from the National Heart, Lung & Blood Institute of the National Institutes of Health.

AUTHOR CONTRIBUTIONS

J.C.S. performed experiments, analyzed data, and wrote the manuscript. S.A.S., A.S., Y.W., R.J.T., and R.H. performed experiments, analyzed data, and participated in the writing of the manuscript. J.H.M. designed and supervised the study, analyzed data, and wrote the manuscript.

RELATIONSHIP DISCLOSURE

There are no competing interests to disclose.

ORCID

James H. Morrissey https://orcid.org/0000-0002-1570-1569

X

Josepha C. Sedzro @JClaraSe
James H. Morrissey @JHMorrissey

REFERENCES

[1] Chan NC, Weitz JI. Antithrombotic agents. *Circ Res*. 2019;124:426–36.
[2] Vappala S, Smith SA, Kizhakkedathu JN, Morrissey JH. Inhibitors of polyphosphate and neutrophil extracellular traps. *Semin Thromb Hemost*. 2023. https://doi.org/10.1055/s-0043-1768936. Online ahead of print.
[3] Ruiz FA, Lea CR, Oldfield E, Docampo R. Human platelet dense granules contain polyphosphate and are similar to acidocalcisomes of bacteria and unicellular eukaryotes. *J Biol Chem*. 2004;279:44250–7.
[4] Moreno-Sanchez D, Hernandez-Ruiz L, Ruiz FA, Docampo R. Polyphosphate is a novel pro-inflammatory regulator of mast cells and is located in acidocalcisomes. *J Biol Chem*. 2012;287:28435–44.
[5] Rao NN, Gómez-García MR, Kornberg A. Inorganic polyphosphate: essential for growth and survival. *Annu Rev Biochem*. 2009;78:605–47.

[6] Smith SA, Mutch NJ, Baskar D, Rohloff P, Docampo R, Morrissey JH. Polyphosphate modulates blood coagulation and fibrinolysis. *Proc Natl Acad Sci U S A*. 2006;103:903–8.

[7] Müller F, Mutch NJ, Schenk WA, Smith SA, Esterl L, Spronk HM, et al. Platelet polyphosphates are proinflammatory and procoagulant mediators *in vivo*. *Cell*. 2009;139:1143–56.

[8] Choi SH, Smith SA, Morrissey JH. Polyphosphate is a cofactor for the activation of factor XI by thrombin. *Blood*. 2011;118:6963–70.

[9] Geng Y, Verhamme IM, Smith SB, Sun M-F, Matafonov A, Cheng Q, et al. The dimeric structure of factor XI and zymogen activation. *Blood*. 2013;121:3962–9.

[10] Smith SA, Morrissey JH. Polyphosphate enhances fibrin clot structure. *Blood*. 2008;112:2810–6.

[11] Mutch NJ, Engel R, Uitte de Willige S, Philippou H, Ariëns RAS. Polyphosphate modifies the fibrin network and down-regulates fibrinolysis by attenuating binding of tPA and plasminogen to fibrin. *Blood*. 2010;115:3980–8.

[12] Smith SA, Choi SH, Davis-Harrison R, Huyck J, Boettcher J, Rienstra CM, et al. Polyphosphate exerts differential effects on blood clotting, depending on polymer size. *Blood*. 2010;116:4353–9.

[13] Ghosh S, Shukla D, Suman K, Lakshmi BJ, Manorama R, Kumar S, et al. Inositol hexakisphosphate kinase 1 maintains hemostasis in mice by regulating platelet polyphosphate levels. *Blood*. 2013;122:1478–86.

[14] Jain S, Pitoc GA, Holl EK, Zhang Y, Borst L, Leong KW, et al. Nucleic acid scavengers inhibit thrombosis without increasing bleeding. *Proc Natl Acad Sci U S A*. 2012;109:12938–43.

[15] Smith SA, Choi SH, Collins JN, Travers RJ, Cooley BC, Morrissey JH. Inhibition of polyphosphate as a novel strategy for preventing thrombosis and inflammation. *Blood*. 2012;120:5103–10.

[16] Travers RJ, Shenoi RA, Kalathottukaren MT, Kizhakkedathu JN, Morrissey JH. Nontoxic polyphosphate inhibitors reduce thrombosis while sparing hemostasis. *Blood*. 2014;124:3183–90.

[17] La CC, Smith SA, Vappala S, Adili R, Luke CE, Abbina S, et al. Smart thrombosis inhibitors without bleeding side effects via charge tunable ligand design. *Nat Commun*. 2023;14:2177. https://doi.org/10.1038/s41467-023-37709-0

[18] Shenoi RA, Kalathottukaren MT, Travers RJ, Lai BFL, Creagh AL, Lange D, et al. Affinity-based design of a synthetic universal reversal agent for heparin anticoagulants. *Sci Transl Med*. 2014;6:260ra150. https://doi.org/10.1126/scitranslmed.3009427

[19] Levêque D, Wisniewski S, Jehl F. Pharmacokinetics of therapeutic monoclonal antibodies used in oncology. *Anticancer Res*. 2005;25:2327–43.

[20] Dubois EL, Horowitz RE, Demopoulos HB, Teplitz R. NZB/NZW mice as a model of systemic lupus erythematosus. *JAMA*. 1966;195:285–9.

[21] Smith SA, Gajsiewicz JM, Morrissey JH. Ability of polyphosphate and nucleic acids to trigger blood clotting: some observations and caveats. *Front Med (Lausanne)*. 2018;5:107. https://doi.org/10.3389/fmed.2018.00107

[22] Baker CJ, Smith SA, Morrissey JH. Diversification of polyphosphate end-labeling via bridging molecules. *PLoS One*. 2020;15:e0237849. https://doi.org/10.1371/journal.pone.0237849

[23] Smith SA, Wang Y, Morrissey JH. DNA ladders can be used to size polyphosphate resolved by polyacrylamide gel electrophoresis. *Electrophoresis*. 2018;39:2454–9.

[24] Stearns DJ, Kurosawa S, Sims PJ, Esmon NL, Esmon CT. The interaction of a Ca^{2+}-dependent monoclonal antibody with the protein C activation peptide region. Evidence for obligatory Ca^{2+} binding to both antigen and antibody. *J Biol Chem*. 1988;263:826–32.

[25] Makishima F, Terada S, Mikami T, Suzuki E. Interleukin-6 is antiproliferative to a mouse hybridoma cell line and promotive for its antibody productivity. *Cytotechnology*. 1992;10:15–23.

[26] Smith SA, Morrissey JH. Polyphosphate as a general procoagulant agent. *J Thromb Haemost*. 2008;6:1750–6.

[27] Hogwood J, Pitchford S, Mulloy B, Page C, Gray E. Heparin and non-anticoagulant heparin attenuate histone-induced inflammatory responses in whole blood. *PLoS One*. 2020;15:e0233644. https://doi.org/10.1371/journal.pone.0233644

[28] Moreau T, Baranger K, Dadé S, Dallet-Choisy S, Guyot N, Zani ML. Multifaceted roles of human elafin and secretory leukocyte proteinase inhibitor (SLPI), two serine protease inhibitors of the chelonianin family. *Biochimie*. 2008;90:284–95.

[29] Faller B, Mely Y, Gerard D, Bieth JG. Heparin-induced conformational change and activation of mucus proteinase inhibitor. *Biochemistry*. 1992;31:8285–90.

[30] Masuda K, Kamimura T, Watanabe K, Suga T, Kanesaki M, Takeuchi A, et al. Pharmacological activity of the C-terminal and N-terminal domains of secretory leukoprotease inhibitor *in vitro*. *Br J Pharmacol*. 1995;115:883–8.

[31] Walter M, Plotnick M, Schechter NM. Inhibition of human mast cell chymase by secretory leukocyte proteinase inhibitor: enhancement of the interaction by heparin. *Arch Biochem Biophys*. 1996;327:81–8.

[32] Schenk JA, Fettke J, Lenz C, Albers K, Mallwitz F, Gajovic-Eichelmann N, et al. Secretory leukocyte protease inhibitor (SLPI) might contaminate murine monoclonal antibodies after purification on protein G. *J Biotechnol*. 2012;158:34–5.

[33] Labberton L, Kenne E, Long AT, Nickel KF, Di Gennaro A, Rigg RA, et al. Neutralizing blood-borne polyphosphate *in vivo* provides safe thromboprotection. *Nat Commun*. 2016;7:12616. https://doi.org/10.1038/ncomms12616

[34] Garcés P, Amaro A, Montecino M, van Zundert B. Inorganic polyphosphate: from basic research to diagnostic and therapeutic opportunities in ALS/FTD. *Biochem Soc Trans*. 2024;52:123–35.

[35] Mailer RKW, Hänel L, Allende M, Renné T. Polyphosphate as a target for interference with inflammation and thrombosis. *Front Med (Lausanne)*. 2019;6:76. https://doi.org/10.3389/fmed.2019.00076

[36] Lorenzo-Orts L, Hohmann U, Zhu J, Hothorn M. Molecular characterization of CHAD domains as inorganic polyphosphate-binding modules. *Life Sci Alliance*. 2019;2:e201900385. https://doi.org/10.26508/lsa.201900385

[37] Cockx M, Van Hoovels L, De Langhe E, Lenaerts J, Thevissen K, Persy B, et al. Laboratory evaluation of anti-dsDNA antibodies. *Clin Chim Acta*. 2022;528:34–43.

[38] Dorai H, Li K, Huang CC, Bittner A, Galindo J, Carmen A. Genome-wide analysis of mouse myeloma cell lines expressing therapeutic antibodies. *Biotechnol Prog*. 2007;23:911–20.

[39] Jin F, Nathan CF, Radzioch D, Ding A. Lipopolysaccharide-related stimuli induce expression of the secretory leukocyte protease inhibitor, a macrophage-derived lipopolysaccharide inhibitor. *Infect Immun*. 1998;66:2447–52.

[40] Schwart W, Judd D, Wysocki M, Guerrier L, Birck-Wilson E, Boschetti E. Comparison of hydrophobic charge induction chromatography with affinity chromatography on protein A for harvest and purification of antibodies. *J Chromatogr A*. 2001;908:251–63.

[41] McDonald B, Davis RP, Kim SJ, Tse M, Esmon CT, Kolaczkowska E, et al. Platelets and neutrophil extracellular traps collaborate to promote intravascular coagulation during sepsis in mice. *Blood*. 2017;129:1357–67. https://doi.org/10.1182/blood.2021014436. Erratum in: Blood 2022;139:952.

SUPPLEMENTARY MATERIAL

The online version contains supplementary material available at https://doi.org/10.1016/j.rpth.2024.102550